



HAL
open science

DFT Analysis into the Calcium(II)-Catalyzed Coupling of Alcohols With Vinylboronic acids: Cooperativity of Two Different Lewis Acids and Counterion Effects

Shengwen Yang, Christophe Bour, David Lebœuf, Vincent Gandon

► To cite this version:

Shengwen Yang, Christophe Bour, David Lebœuf, Vincent Gandon. DFT Analysis into the Calcium(II)-Catalyzed Coupling of Alcohols With Vinylboronic acids: Cooperativity of Two Different Lewis Acids and Counterion Effects. *Journal of Organic Chemistry*, 2021, 86 (13), pp.9134-9144. <10.1021/acs.joc.1c01263>. <hal-03401941>

HAL Id: hal-03401941

<https://hal.science/hal-03401941v1>

Submitted on 25 Oct 2021

HAL is a multi-disciplinary open access archive for the deposit and dissemination of scientific research documents, whether they are published or not. The documents may come from teaching and research institutions in France or abroad, or from public or private research centers.

L'archive ouverte pluridisciplinaire HAL, est destinée au dépôt et à la diffusion de documents scientifiques de niveau recherche, publiés ou non, émanant des établissements d'enseignement et de recherche français ou étrangers, des laboratoires publics ou privés.



HAL Authorization

DFT Analysis into the Calcium(II)-Catalyzed Coupling of Alcohols With Vinylboronic acids: Cooperativity of Two Different Lewis Acids and Counterion Effects.

Shengwen Yang,^{†,‡} Christophe Bour,[†] David Leboeuf,^{†,‡,‡} Vincent Gandon^{},^{†,‡}*

[†]Institut de Chimie Moléculaire et des Matériaux d'Orsay (ICMMO), CNRS UMR 8182, Université Paris-Sud, Université Paris-Saclay, Bâtiment 420, 91405 Orsay cedex, France.

[‡]Laboratoire de Chimie Moléculaire (LCM), CNRS UMR 9168, Ecole Polytechnique, Institut Polytechnique de Paris, route de Saclay, 91128 Palaiseau cedex, France.

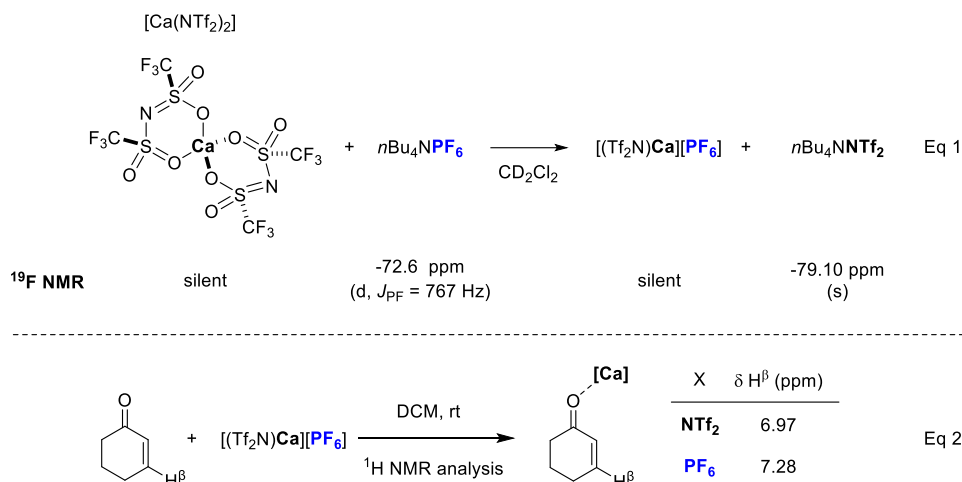
[‡]Institut de Science et d'Ingénierie Supramoléculaires (ISIS), CNRS UMR 7006, Université de Strasbourg, 67000 Strasbourg, France.

KEYWORDS. Calcium, Superelectrophiles, Alcohols, Vinylboronic Acids, Coupling Reactions, DFT.

ABSTRACT. The mechanism of the calcium-catalyzed coupling of alcohols with vinylboronic acids has been analyzed by means of DFT computations. This study reveals that the calcium and the boron Lewis acids associate to form a superelectrophile able to promote a pericyclic group

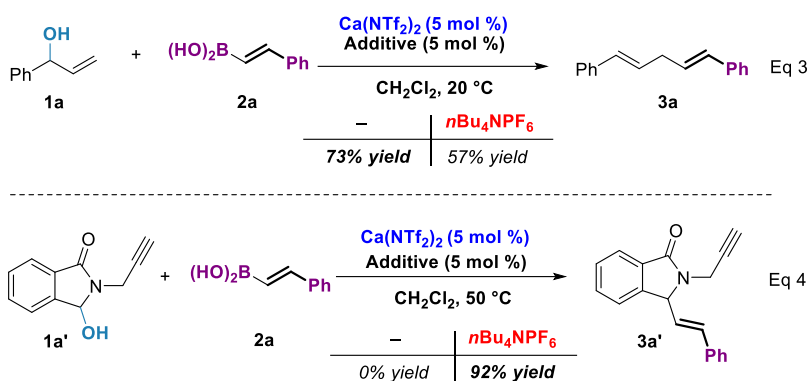
transfer reaction with allyl alcohols. With other alcohols, the two Lewis acids act synergistically to activate the OH functionality and trigger a S_Ni reaction pathway. These two mechanisms are affected by the nature of the counterions, which has been rationalized by electronic and steric factors.

INTRODUCTION. Since a decade, calcium-based Lewis acids have witnessed an upsurge of applications in homogeneous catalysis. This renaissance was mostly led by the group of Niggemann who reported that $\text{Ca}(\text{NTf}_2)_2$ can be activated by an ammonium salt of a weakly coordinating anion such as $n\text{Bu}_4\text{NPF}_6$ to give a highly oxophilic Lewis acid able to abstract hydroxy groups and promote cationic transformations.^{1,2} This strategy is also efficient with $\text{Ca}(\text{OTf})_2$.³ Other functional groups can also be activated, such as ketones or alkenes.⁴ The structure of $\text{Ca}(\text{NTf}_2)_2 \cdot 4\text{H}_2\text{O}$ was reported in 2005 and shows that the calcium ion is not bound to the nitrogen atom of the NTf_2^- counterion, but to the oxygen atoms of the SO_2CF_3 moiety adopting a *cis* configuration of the CF_3 groups (Scheme 1, Eq 1).⁵ This relationship between the metal and its counterions is in sharp contrast with soft transition metals that are usually coordinated to the nitrogen atom, and it reveals the strong oxophilicity of calcium. Thus, $\text{Ca}(\text{NTf}_2)_2$ is not a very strong Lewis acid since the counterions are strongly coordinated and occupy 4 coordination sites of the metal. On the other hand, a mixture of $\text{Ca}(\text{NTf}_2)_2$ and $n\text{Bu}_4\text{NPF}_6$ has a more pronounced Lewis acidity, as shown by the NMR Childs' test (Scheme 1, Eq 2).^{4b} Indirect spectroscopic evidence based on the disappearance of the ^{19}F NMR signals of the spinning counterions attached to the metal center suggested the formation of $[\text{Ca}(\text{NTf}_2)]^+[\text{PF}_6]^-$ (Scheme 1, Eq 1).^{4b,6} The driving force of this anion metathesis, during which a strongly coordinated anion (NTf_2^- or OTf) is replaced by a weakly coordinating one (PF_6^-) might be due to a higher solubility of the heteroleptic species.



Scheme 1. $\text{Ca}(\text{NTf}_2)_2$ and $[(\text{Tf}_2\text{N})\text{Ca}][\text{PF}_6]$

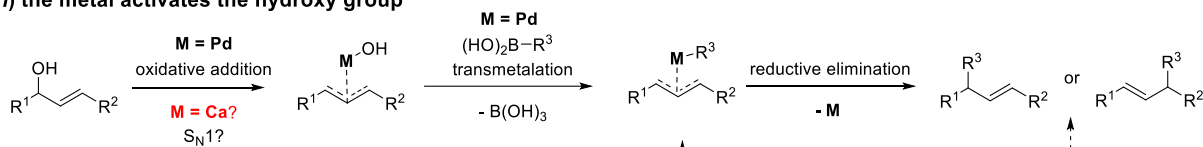
The mixture composed of $\text{Ca}(\text{NTf}_2)_2$ and $n\text{Bu}_4\text{NPF}_6$ or other $[\text{R}_4\text{N}]^+[\text{WCA}]^-$ species (WCA = weakly coordinating anion) proved particularly efficient for catalyzing the nucleophilic substitution of alcohols, a process that is believed to follow a $\text{S}_{\text{N}}1$ pathway.^{1a} As far as we are concerned, we have developed the calcium-catalyzed coupling of alcohols with vinylboronic acids (Scheme 2).⁷ This alkenylation reaction is efficient towards allyl-, benzyl- and propargyl alcohols (Eq 3),^{7a} as well as *N,O*-acetals (Eq 4).^{7b} While the positive effect of the ammonium salt was obvious with *N,O*-acetal **1a'**, a better yield was actually obtained in its absence with allyl alcohol **1a**. Besides, for alcohols such as **1a**, the structure of the product **3a** does not suggest a $\text{S}_{\text{N}}1$ reaction but rather a $\text{S}_{\text{N}}2'$ process.



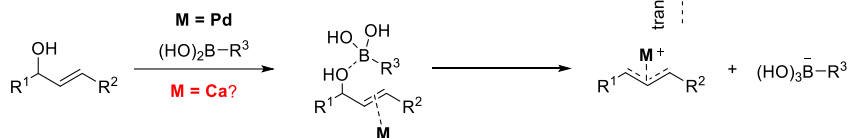
Scheme 2. Calcium-Catalyzed Alkenylation of Alcohols.

To rationalize these experimental results, we decided to explore the mechanism of these two coupling reactions by DFT calculations.⁸ Of course, most data available on the cross-coupling of allyl alcohols with vinylboronic acids are related to palladium catalysis (Scheme 3). The reaction might start with the oxidative addition of palladium to produce a π -allylpalladium intermediate by direct activation of the hydroxy group (*i*).⁹ Alternatively, the hydroxy group of the allyl alcohol can be activated by the boronic acid to facilitate the oxidative addition (*ii*).¹⁰ With calcium, while these two activation modes can be envisaged, we also considered in this study the synergistic activation of the hydroxy group by the two Lewis acids (Ca and B) (*iii*).

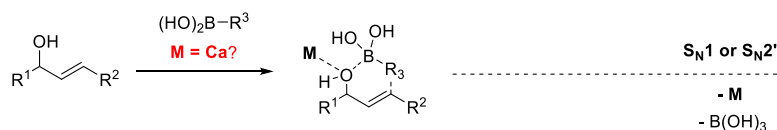
i) the metal activates the hydroxy group



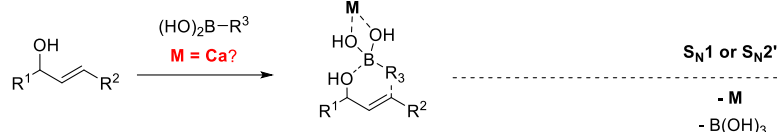
ii) Boronic acid activates the hydroxy group



iii) Calcium and boronic acid synergistically activate the hydroxy group



iv) Calcium activates boronic acid which activates the hydroxy group



Scheme 3. Mechanistic Hypotheses.

A last possibility would be a Lewis acid activation of the boronic acid itself by coordination of the calcium salt to the oxygen atoms of the boronic acid (iv). We have shown in the past that the calcium(II) ion can strengthen the acidity of Brønsted acids such as hexafluoroisopropanol (HFIP),¹¹ which triggers reactions such as the hydroamidation^{4c} or the hydroarylation of alkenes.^{4d} Herein, the principle of activation of an electrophile (B) by another electrophile (Ca) through heterodimeric association, leading to a superelectrophile,^{12,13} is revisited and the role of the counterions is analyzed.

RESULTS AND DISCUSSION

1. Mechanism of the Calcium(II)-Catalyzed Alkenylation of Allylbenzyl Alcohol 1a with (*E*)-Styrylboronic Acid 2a.

1.1. Activation of the Hydroxy Group by Calcium (S_N1). The feasibility of the above proposed mechanism (Scheme 3, (i)) was first examined (Figure 1). There are two reaction zero points considering that both $\text{Ca}(\text{NTf}_2)_2$ and $\text{Ca}(\text{NTf}_2)(\text{PF}_6)$ can be active catalysts depending on the use of $n\text{Bu}_4\text{NPF}_6$ as additive.

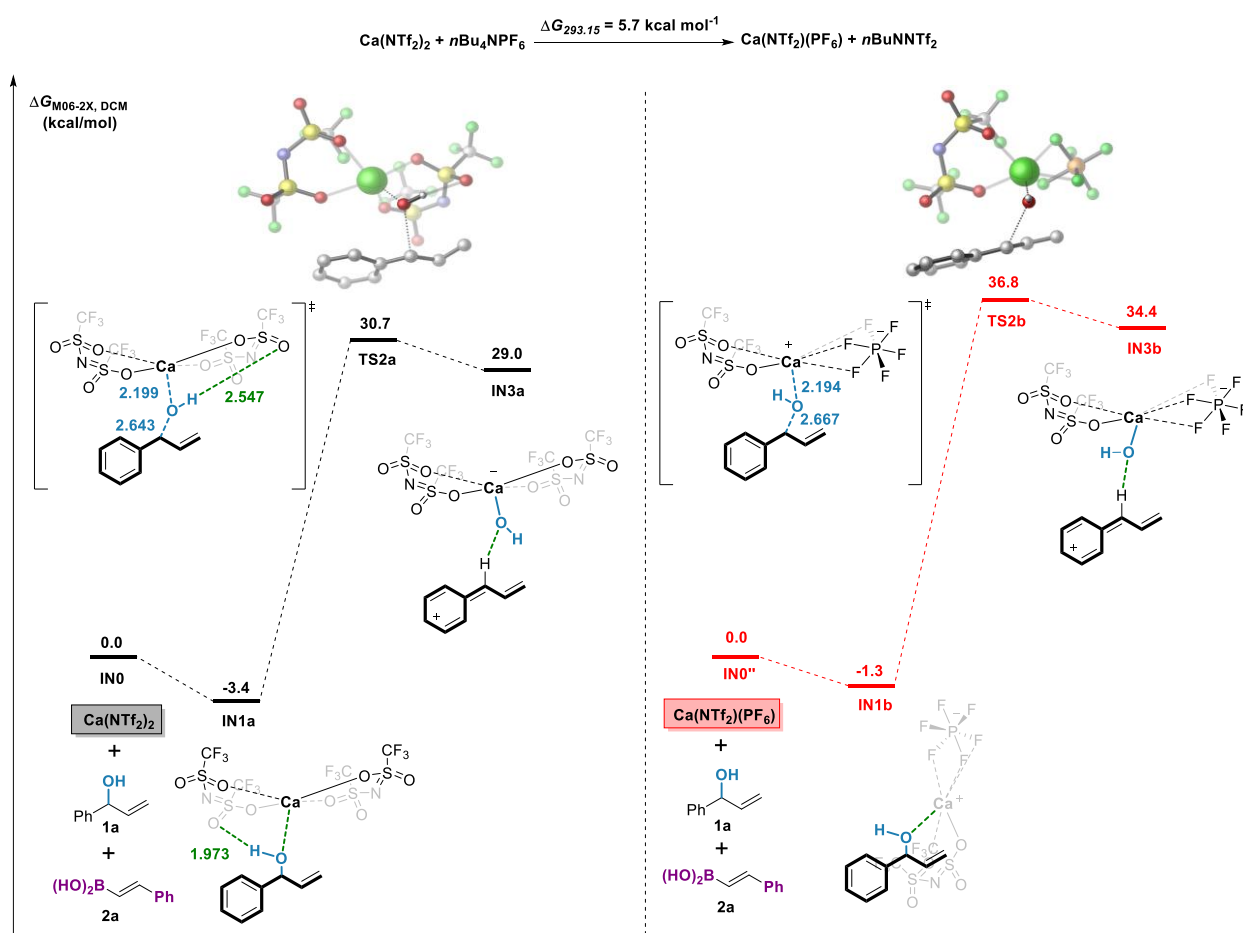


Figure 1. Free Energy Profile (kcal mol^{-1}) for the Calcium-Mediated Hydroxy Group Abstraction. Selected Distances in Å.

The coordination of the hydroxy group of alcohol **1a** to $\text{Ca}(\text{NTf}_2)_2$ to provide complex **IN1a** is exergonic by $3.4 \text{ kcal mol}^{-1}$. There is a hydrogen bond between one sulfonyl oxygen and the OH group ($\text{S}=\text{O}\cdots\text{H}-\text{O}$ 1.973 \AA) which disappears in the subsequent transition state and product. The cleavage of the C–O bond must overcome a barrier of $34.1 \text{ kcal mol}^{-1}$ through transition state **TS2a**. This process is markedly endergonic by $32.4 \text{ kcal mol}^{-1}$ (**IN3a**). In spite of its stronger Lewis acidity (Scheme 1, Eq 2), $\text{Ca}(\text{NTf}_2)(\text{PF}_6)$ leads to an even higher barrier of $38.1 \text{ kcal mol}^{-1}$ from **IN1b** to provide **IN3b** in a strongly endergonic fashion ($34.4 \text{ kcal mol}^{-1}$). With such high free energies of activation, this type of $\text{S}_{\text{N}}1$ mechanism was not considered any further.

1.2. Activation of the Hydroxy Group by (E)-Styrylboronic Acid ($\text{S}_{\text{N}}1$). Next, we evaluated a pathway corresponding to (ii) in Scheme 3 (Figure 2). The activation free energies of the hydroxy abstraction are $61.5 \text{ kcal mol}^{-1}$ (**TS2c**) and $70.9 \text{ kcal mol}^{-1}$ (**TS2d**) with $\text{Ca}(\text{NTf}_2)_2$ and $\text{Ca}(\text{NTf}_2)(\text{PF}_6)$, respectively. This is, therefore, a very unlikely mechanism.

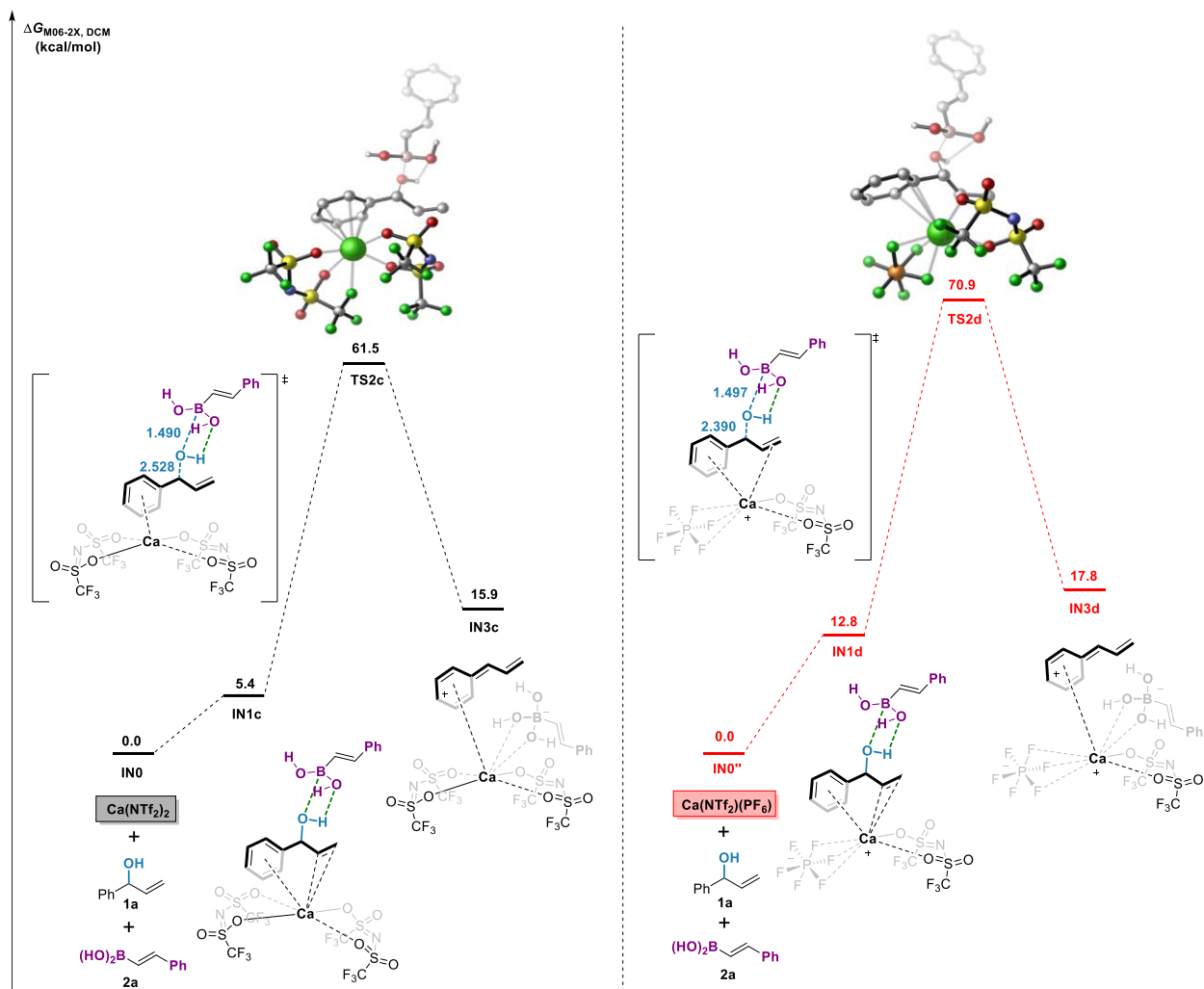


Figure 2. Free Energy Profile (kcal mol^{-1}) for (*E*)-Styrylboronic Acid-Mediated Hydroxy Group Abstraction. Selected Distances in Å.

1.3. *Attempted Hydroxy Group Activation by the Two Lewis Acids (Ca/B).* According to pathway (iii) proposed in Scheme 3, we studied the dual activation of the hydroxy group by the calcium complex and the vinylboronic acid. However, it was not possible to accommodate the two Lewis acids on the same oxygen donor atom with this substrate. The species converged as **IN1** (see Figure 3) in which calcium is coordinated to an OH group of the boronic acid, leading to the following discussion (Section 1.4).

1.4. Lewis Acid Activation of the Boronic Acid (*Ca/B*; formal S_N2'). The formation of **IN1** from $\text{Ca}(\text{NTf}_2)_2$, **1a** and **2a** is exergonic by $1.0 \text{ kcal mol}^{-1}$ (Figure 3). Two oxygen atoms of **2a** are coordinated to the calcium center. The oxygen atom of **1a** is coordinated by the boron center and is bound to the calcium salt through a hydrogen bond involving the NTf_2^- counterion ($\text{S}=\text{O}\cdots\text{H}-\text{O}$ 1.889 \AA). Trying to cleave the C–O bond of **1a** actually led to the concomitant formation of a C–C bond through the six-membered ring transition state **TS2**, which requires a reasonable activation energy of $20.2 \text{ kcal mol}^{-1}$ relatively to **IN1**.

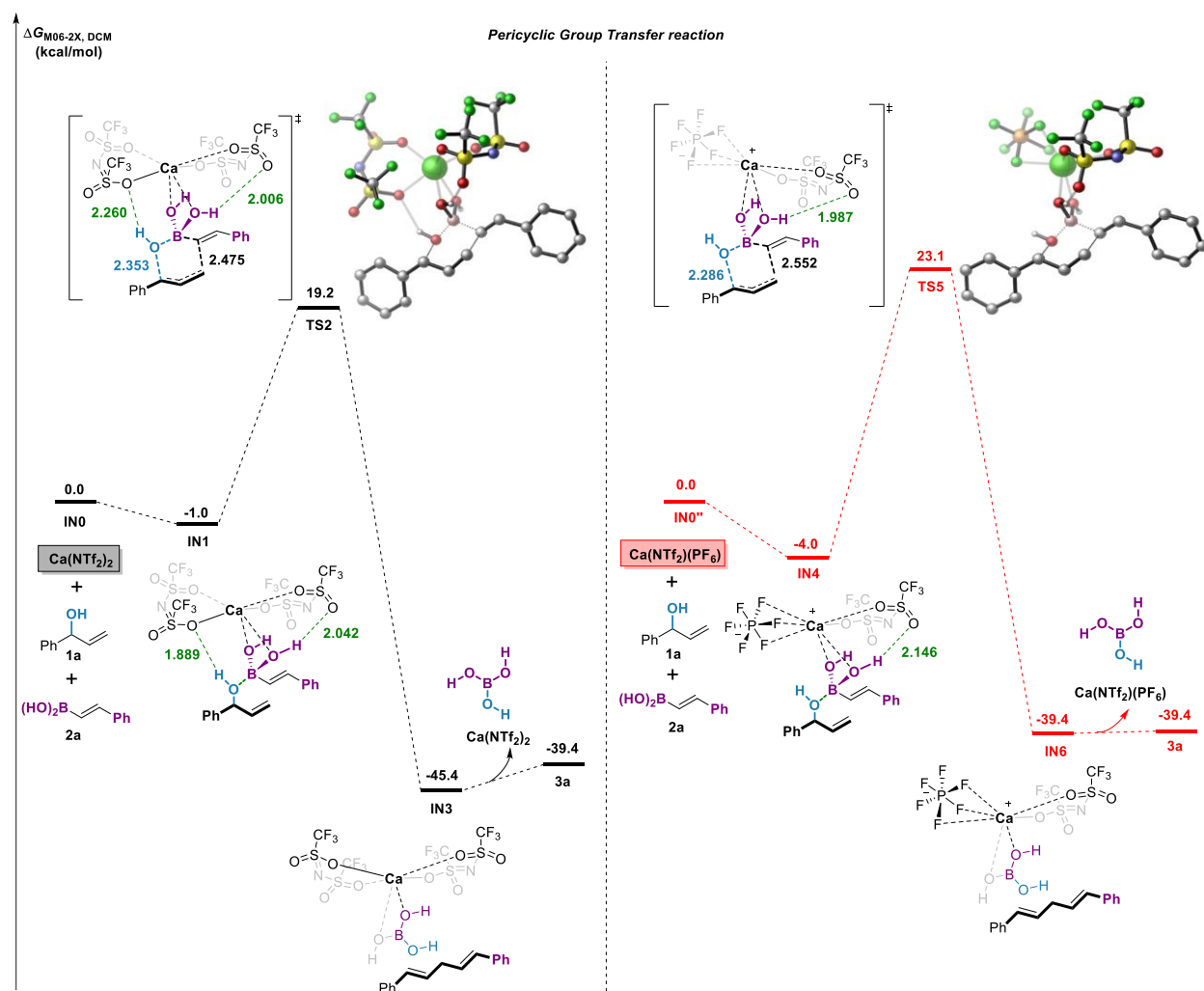


Figure 3. Free Energy Profile (kcal mol^{-1}) for the Concerted Ca/B-Mediated Hydroxy Group Abstraction/Vinylation. Selected distances in Å.

This process is markedly exergonic by $44.4 \text{ kcal mol}^{-1}$ and gives **IN3**. Elimination of B(OH)_3 and $\text{Ca(NTf}_2)_2$ finally leads to the final product **3a** lying at $-39.4 \text{ kcal mol}^{-1}$.

At this stage, two important features are worth emphasizing:

1- The geometry of **TS2** and the FMO analysis of its fragment clearly shows that it corresponds to a **pericyclic *suprafacial/suprafacial* group transfer reaction** (Figure 4).¹⁴ To the best of our knowledge, such a group transfer reaction has not been described before.

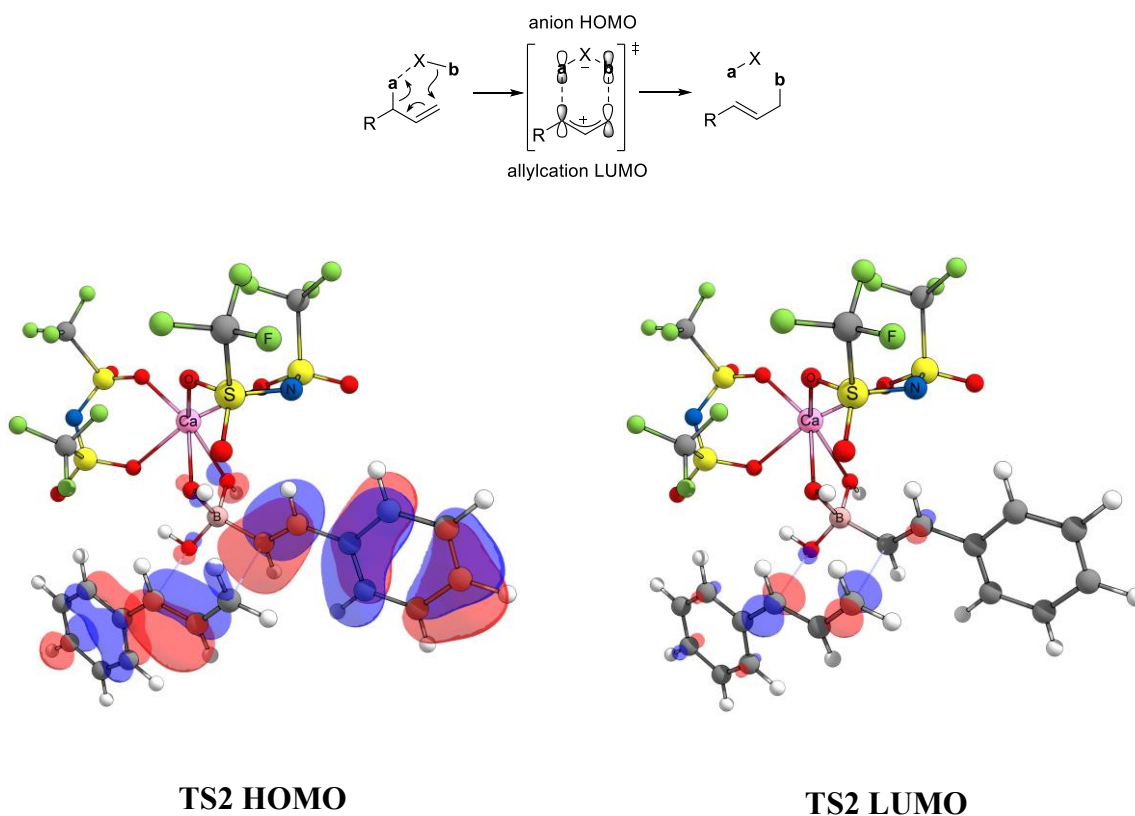
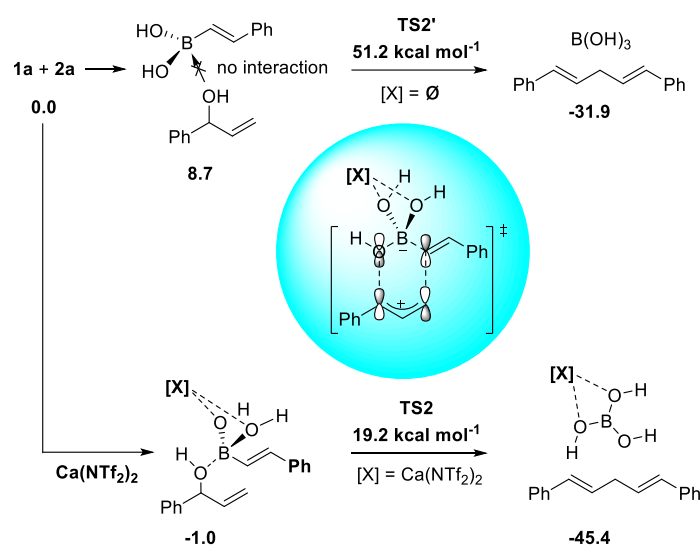


Figure 4. Prototype of the Pericyclic Group Transfer Reaction and FMO analysis of **TS2**.

2- In the absence of $\text{Ca}(\text{NTf}_2)_2$, the barrier to reach the same kind of 6-membered ring transition state becomes **51.2 kcal mol⁻¹** (Scheme 4), which reveals the crucial role of the catalyst in activating the boron Lewis acid. The interaction between **1a** and **2a** cannot even be modeled if the calcium is not bound to the OH groups of the boronic acid (virtually planar $\text{RB}(\text{OH})_2$ moiety vs pyramidal boron center in **IN1**), showing that its role is to strengthen the electrophilicity of the boron reagent.



Scheme 4. Effect of Calcium Coordination to the Boronic Acid on the Pericyclic Group Transfer Reaction

With the $\text{Ca}(\text{NTf}_2)(\text{PF}_6)$ species, in agreement with the experimental results, the barrier to reach the same kind of 6-membered ring transition state is markedly higher (Figure 3, right). The free energy difference between **IN4** and **TS5** is 27.1 kcal mol⁻¹, versus 20.2 with $\text{Ca}(\text{NTf}_2)_2$. Of note, inverting the position of the PF_6^- and the NTf_2^- ions led to an even higher-lying transition state (30.8 kcal mol⁻¹ instead of 27.1 kcal mol⁻¹, see Figure S1 in the Supporting Information). We have carefully analyzed the hydrogen bonds between the NTf_2^- oxygen atoms and the various OH

groups of the two substrates (**1a** and **2a**). The strongest ones are indicated in Figure 3. Even though there are less possibilities of such noncovalent interactions with the $\text{Ca}(\text{NTf}_2)(\text{PF}_6)$ fragment compared to $\text{Ca}(\text{NTf}_2)_2$, we could not explain the difference of efficiency between these two active species on the basis of hydrogen bonding. With the seemingly more electrophilic $\text{Ca}(\text{NTf}_2)(\text{PF}_6)$ species, the coordinated boronic acid is also more electrophilic and this facilitates the OH abstraction. However, the nucleophilicity of the vinyl group is also a crucial factor. With a more electrophilic calcium activator, the vinyl group will be less nucleophilic. This transpires in the geometry of the transition states as well, the forming C–C being longer in **TS5** than in **TS2** (2.552 vs 2.475 Å). The natural charges confirm this trend (Figure 4), with for instance the q_C charge, which is more negative with $\text{Ca}(\text{NTf}_2)_2$ than with $\text{Ca}(\text{NTf}_2)(\text{PF}_6)$ (-0.453 vs -0.447 e). Thus, the right balance must be found to efficiently activate the boronic acid while maintaining its nucleophilicity. This is why the reaction of **1a** with **2a** is more efficient with $\text{Ca}(\text{NTf}_2)_2$ than with $\text{Ca}(\text{NTf}_2)(\text{PF}_6)$. The fact that the reaction does not obey a $\text{S}_{\text{N}}1$ mechanism but a concerted group transfer explains why a less electrophilic activator is a better option in this case.

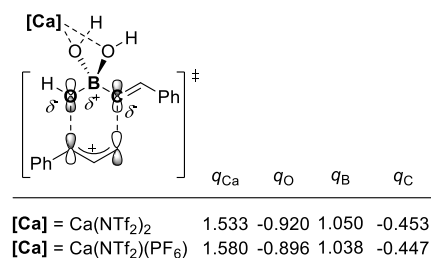


Figure 4. NPA charges of **TS2** ($[\text{Ca}] = \text{Ca}(\text{NTf}_2)_2$) and **TS5** ($[\text{Ca}] = \text{Ca}(\text{NTf}_2)(\text{PF}_6)$).

2. Mechanism of the Calcium(II)-Catalyzed Alkenylation of 3-Hydroxyisoindolinone **1a'** with (*E*)-Styrylboronic Acid **2a**.

2.1. *Activation of the Hydroxy Group by Calcium (S_N1)*. Similarly to the results obtained in the first section, OH abstraction faces very high barriers (Figure 5): 34.8 kcal mol⁻¹ with Ca(NTf₂)₂; 36.1 kcal mol⁻¹ with Ca(NTf₂)(PF₆). The S_N1 mechanism is therefore also ruled out for 3-hydroxyisindolinone.

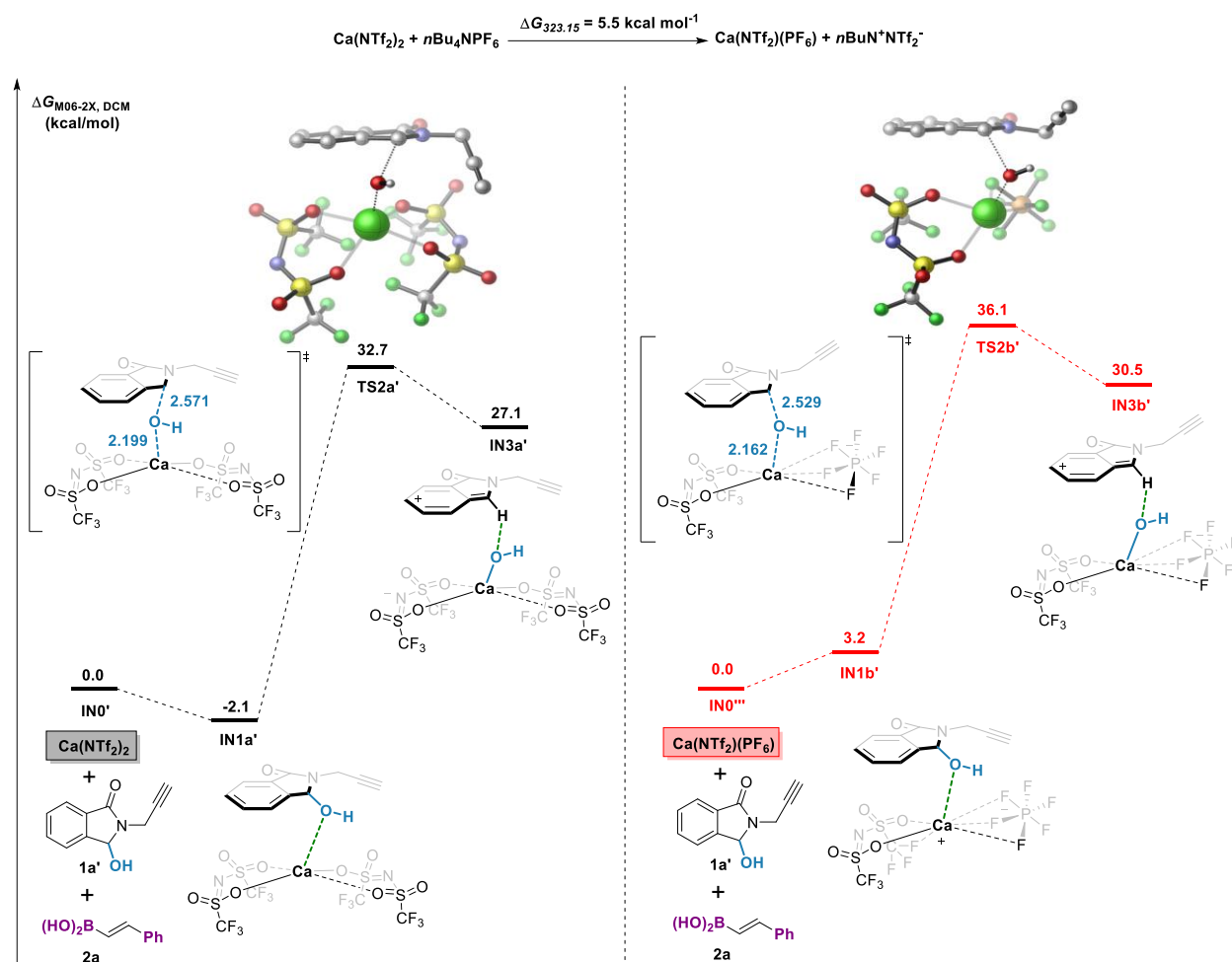


Figure 5. Free Energy Profile (kcal mol⁻¹) for the Calcium-Mediated Hydroxy Group Abstraction. Selected distances in Å.

2.2. *Activation of the Hydroxy Group by (E)-Styrylboronic Acid (S_N1)*. Due to the very large barriers computed in Section 1.2, this type of activation was not studied.

2.3. *Hydroxy Group Activation by the Two Lewis Acids (Ca/B; S_N1)*. Again, it was not possible to accommodate the two metals on the OH group of the substrate.

2.4. *Lewis Acid Activation of the Boronic Acid (Ca/B; S_Ni)*. Coordination of 3-hydroxyisoindolinone **1a'** and (*E*)-styrylboronic acid **2a** to calcium center provides complex **IN1'**, lying 2.0 kcal mol⁻¹ below the reactants **IN0'** (Figure 6). There is not interaction between the OH group of **1a'** and the boron center at this stage, but while the C–O bond breaks, the OH group directly migrates to boron and not to calcium. This step through **TS2'** requires a free energy of activation of 21.1 kcal mol⁻¹ from **IN1'** and is endergonic by 14.6 kcal mol⁻¹. The vinyl group is then delivered from the intimate ion pair **IN3'** to **IN5'** in a strongly exergonic fashion. The corresponding transition state **TS4'** culminates at 28.2 kcal mol⁻¹ on the free energy surface. Finally, the Ca(NTf₂)₂ is regenerated with concomitant release of B(OH)₃ and product **3a'**, which is 31.0 kcal mol⁻¹ below the reactants. Overall, this process needs to overcome an energy barrier as high as 30.2 kcal mol⁻¹, which is consistent with the experimental results in which no product was observed (Scheme 2, Eq 4). On the other hand, 92% yield was obtained with the use of *n*Bu₄NPF₆. The corresponding mechanism is shown by the red line in Figure 6. Coordination of 3-hydroxyisoindolinone **1a'** and (*E*)-styrylboronic acid **2a** to the calcium center is slightly endergonic, placing the resulting intermediate **IN6'** at 3.9 kcal mol⁻¹ on the free energy surface. Hydroxy group migration to boron to generate the ion pair **IN8'** is achieved through **TS7'**. This step needs to cross an energy barrier of 22.2 kcal mol⁻¹ relatively to **IN0''**. Then, the nucleophilic addition occurs through **TS9'**, located at 25.0 kcal mol⁻¹ on the free energy surface (vs 28.2 kcal mol⁻¹ for **TS4'**). We have also considered other possible hydroxy and counterions orientation, but the corresponding activation energies of these nucleophilic additions were significantly higher (see Figure S3). Finally, the Ca(NTf₂)(PF₆) is regenerated with concomitant release of the desired

product **3a'** and B(OH)_3 . Thus, the best computed mechanism of the vinylation of 3-hydroxyisoindolinones is a **substitution nucleophilic intramolecular (S_{Ni})** going through an ion pair. In such processes, the leaving group and the nucleophile are exchanged on the same side of the substrate.

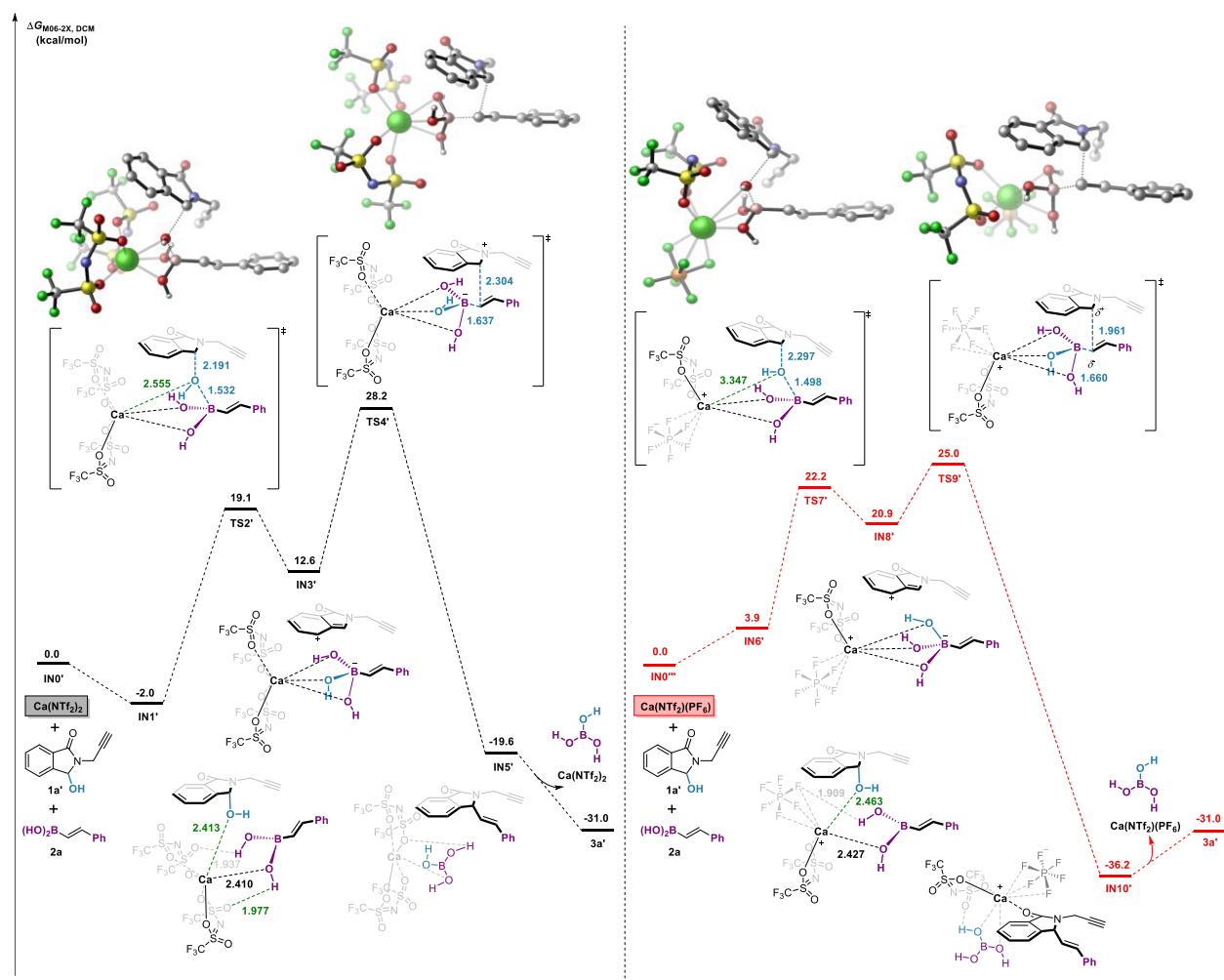


Figure 6. Free Energy Profile (kcal mol^{-1}) for the Ca/B-Mediated Hydroxy Group Abstraction of **1a'**.

To understand the better reactivity conferred by $\text{Ca}(\text{NTf}_2)(\text{PF}_6)$ compared to $\text{Ca}(\text{NTf}_2)_2$, we have used the Global Nucleophilicity (N) proposed by Domingo et al.¹⁵ but no significant difference could be found (see Figure S4). On the other hand, noncovalent interactions analysis (NCIs)¹⁶ of the nucleophilic addition transition states **TS4'** and **TS9'** proved relevant (Figure 7). There is a lone pair repulsion between the oxygen of NTf_2^- ion and the oxygen atom of the isoindolinone cation in transition state **TS4'**, which explains why this structure is more difficult to reach compared to **TS9'**. The proximity between the two oxygen atoms is imposed by the large size of the NTf_2^- ion. With the smaller PF_6^- counterion, the NTf_2^- is far from the carbonyl group.

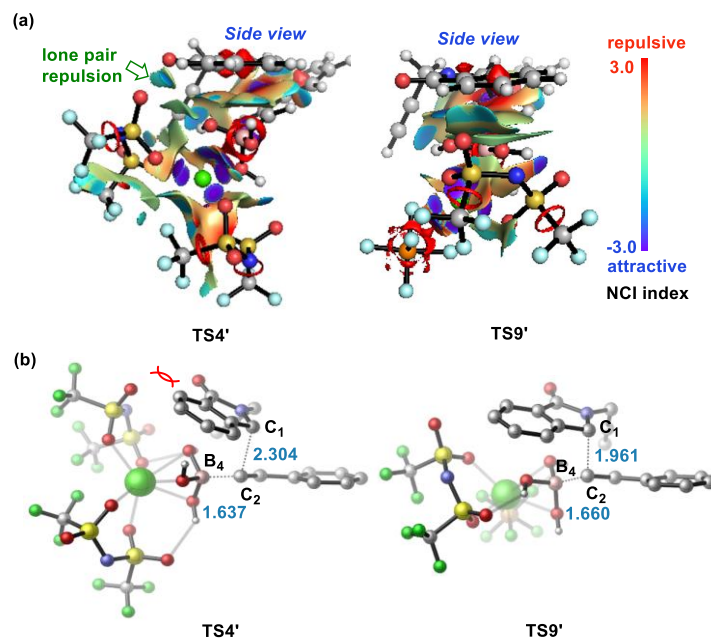
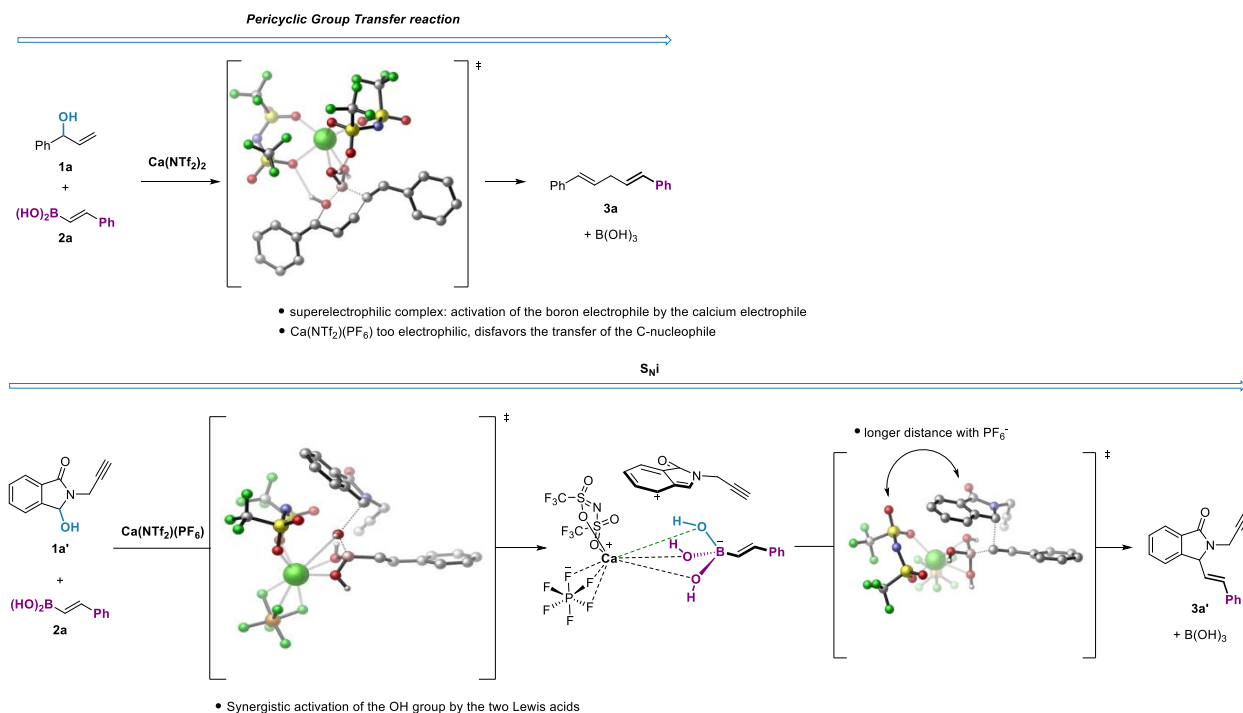


Figure 7. (a) Non-covalent interactions analysis of **TS4'** and **TS9'** (blue, strongly attractive; green, weakly attractive; red, strongly repulsive). (b) Optimized structure of the two transition states. Selected distances in Å.

3. CONCLUSION

The proposed mechanisms of the calcium(II)-catalyzed coupling of alcohols with vinylboronic acids are summarized in Scheme 5. For the reaction of allyl alcohols, the calculations suggest a pericyclic group transfer reaction in which the calcium and the boron Lewis acids form a superelectrophilic complex. The reason why $\text{Ca}(\text{NTf}_2)_2$ is better than $\text{Ca}(\text{NTf}_2)(\text{PF}_6)$ is attributed to the weaker Lewis acidity of the former: in the transition state, the activated boron is rendered electrophilic enough abstract the OH group of the alcohol while the vinyl group remains a good nucleophile. Since $\text{Ca}(\text{NTf}_2)_2$ is a weaker Lewis acid than $\text{Ca}(\text{NTf}_2)(\text{PF}_6)$, its counterion combination represents the best compromise to activate the boron center as a Lewis acid and maintain the nucleophilic character of the vinylboronic acid as a reagent. For alcohols for which a concerted mechanism is no longer possible, such as 3-hydroxyisoindolinones, the DFT study support a S_{NI} -type reaction. The abstraction of the OH group is facilitated by its synergistic activation by the two Lewis acids. Rather than an electronic tuning provided by the counterion, we found that the better activity of the $\text{Ca}(\text{NTf}_2)(\text{PF}_6)$ species is due to the smaller size of the PF_6^- ion compared to NTf_2^- , which avoids a pair repulsion between one of the NTf_2^- oxygen and the carbonyl group of the substrate. Overall, this study sheds light on the cooperativity between two Lewis acids in catalysis and on the counterion effects in such coupling reactions.



Scheme 5. Proposed Mechanisms of the Calcium(II)-Catalyzed Coupling of Alcohols with Vinylboronic Acids

4. COMPUTATIONAL METHODS

We have used the Gaussian 09 set of programs¹⁷ to perform density functional theory (DFT) computations. All structures were optimized and characterized as energy minima or transition states (TS) at the M06-2X¹⁸/6-31G(d) level. The energies were then refined by M06-2X/6-311+G(d,p) single-point calculations including solvation effects of dichloromethane accounted for by the SMD¹⁹ model. The M06-2X hybrid functional has been previously shown to achieve good accuracy for calcium-based systems.^{4c,e} The refined single-point energies were then corrected to enthalpies and free energies at 1 atm and 293.15 K or 323.15 K using the gas phase M06-2X/6-31G(d) harmonic frequencies. We confirmed transition state structures by intrinsic reaction coordinate (IRC) calculations²⁰ to connect the correct reactant/product and intermediates on the

potential energy surface (PES). The values presented are $\Delta G_{293.15}$ (kcal mol⁻¹) or $\Delta G_{323.15}$ (kcal mol⁻¹). The most significant three-dimensional structures are illustrated with CYLview.²¹ Total energies and Cartesian coordinates of all optimized structures are given in the Supporting Information (SI).

ASSOCIATED CONTENT

Supporting Information. Cartesian coordinates and total energies for all optimized geometries are tabulated in the Supporting Information (PDF).

AUTHOR INFORMATION

Corresponding Author

* Email: vincent.gandon@universite-paris-saclay.fr

Author Contributions

The manuscript was written through contributions of all authors. All authors have given approval to the final version of the manuscript.

Notes

The authors declare no competing financial interest.

ACKNOWLEDGMENT

SY thanks the China Scholarship Council (CSC) for PhD grant. We thank the UPSaclay, Ecole Polytechnique, and ANR-18-CE07-0033-01 (HICAT) for financial support of this work. This work was granted access to the HPC resources of CINES under the allocation 2020-A0070810977 made by GENCI.

REFERENCES

1 For reviews on Ca(II) catalysis, see: (a) Begouin, J.-M.; Niggemann, M. Calcium-Based Lewis Acid Catalysts. *Chem. Eur. J.* **2013**, *19*, 8030-8041. (b) Lebœuf, D.; Gandon, V. Carbon-Carbon and Carbon-Heteroatom Bond-Forming Transformations Catalyzed by Calcium(II) Triflimide. *Synthesis* **2017**, *49*, 1500-1508. (c) Rauser, M.; Schröder, S.; Niggemann, M. In *Early Main Group Metal Lewis Acid Catalysis: Concepts and Reactions*; Harder, S., Ed.; Wiley-VCH, **2020**, pp 279-310. (d) Kobayashi, S.; Yamashita, S. Alkaline Earth Metal Catalysts for Asymmetric Reactions. *Acc. Chem. Res.* **2011**, *44*, 58-71. (e) Harder, S. From Limestone to Catalysis: Application of Calcium Compounds as Homogeneous Catalysts. *Chem. Rev.*, **2010**, *110*, 3852-3876.

2 For selected examples of alcohol activation, see: (a) Niggemann, M.; Meel, M. J. Calcium-Catalyzed Friedel-Crafts Alkylation at Room Temperature. *Angew. Chem. Int. Ed.* **2010**, *49*, 3684-3687. (b) Haven, T.; Kubik, G.; Haubenreisser, S.; Niggemann, M. Calcium-Catalyzed Cyclopropanation. *Angew. Chem. Int. Ed.* **2013**, *52*, 4016-4019. (c) Wang, S.; Guillot, R.; Carpentier, J.-F.; Sarazin, Y.; Bour, C.; Gandon, V.; Lebœuf, D. Synthesis of Bridged Tetrahydrobenzo[b]azepines and Derivatives through an Aza-Piancatelli Cyclization/Michael Addition Sequence. *Angew. Chem. Int. Ed.* **2020**, *59*, 1134-1138.

3 See inter alia: (a) Yaragorla, S.; Rajesh, P.; Pareek, A.; Kumar, A. Ca(II)-Mediated Regioselective One-Pot Sequential Annulation of Acyclic compounds to Polycyclic Fluorenopyrans. *Adv. Synth. Catal.* **2018**, *360*, 4422-4428. (b) Yaragorla, S.; Dada, R.; Rajesh, P.; Sharma, M. Highly Regioselective Synthesis of Oxindolyl-Pyrroles and Quinolines via a One-Pot, Sequential Meyer-Schuster Rearrangement, Anti-Michael Addition/C(sp³)-H Functionalization, and Azacyclization. *ACS Omega* **2018**, *3*, 2934-2946.

4 For selected examples: (a) Haubenreisser, S.; Hensenne, P.; Schröder, P. Niggemann, M. *Org. Lett.* **2013**, *15*, 2262-2265. (b) Davies, J.; Leonori, D. The First Calcium-Catalysed Nazarov Cyclisation. *Chem. Commun.* **2014**, *50*, 15171-15174. (c) Qi, C.; Hasenmaile, F.; Gandon, V.; Lebœuf, D. Calcium(II)-Catalyzed Intra- and Intermolecular Hydroamidation of Unactivated Alkenes in Hexafluoroisopropanol. *ACS Catal.* **2018**, *8*, 1734-1739. (d) Qi, C.; Gandon, V.; Lebœuf, D. Calcium(II)-Catalyzed Intermolecular Hydroarylation of Deactivated Styrenes in Hexafluoroisopropanol. *Angew. Chem. Int. Ed.* **2018**, *57*, 14245-14249. (e) Qi, C.; Yang, S.; Gandon, V.; Lebœuf, D. Calcium(II)- and Triflimide-Catalyzed Intramolecular Hydroacyloxylation of Unactivated Alkenes in Hexafluoroisopropanol. *Org. Lett.* **2019**, *21*, 7405-7409. (f) Wang, S.; Force, G.; Guillot, R.; Carpentier, J.-F.; Sarazin, Y.; Bour, C.; Gandon, V.; Leboeuf, D. Lewis Acid/Hexafluoroisopropanol: A Promoter System for Selective ortho-C-Alkylation of Anilines with Deactivated Styrene Derivatives and Unactivated Alkenes. *ACS Catal.* **2020**, *10*, 10794-10802.

5 Xue, L.; DesMarteau, D. D.; Pennington, W. T. Synthesis and Structures of Alkaline Earth Metal Salts of bis[(Trifluoromethyl)sulfonyl]imide. *Solid State Sciences* **2005**, *7*, 311-318.

6 Haubenreisser, S.; Niggemann, M. Calcium-Catalyzed Direct Amination of π -Activated Alcohols. *Adv. Synth. Catal.* **2011**, *353*, 469-474.

7 (a) Lebœuf, D.; Pisset, M.; Michelet, B.; Bour, C.; Bezzenine-Lafollée, S.; Gandon, V. Ca(II)-Catalyzed Alkenylation of Alcohols with Vinylboronic Acids. *Chem. Eur. J.* **2015**, *21*, 11001-11005. (b) Qi, C.; Gandon, V.; Leboeuf, D. Calcium(II)-Catalyzed Alkenylation of N-Acyliminiums and Related Ions with Vinylboronic Acids. *Adv. Synth. Catal.* **2017**, *359*, 2671-2675.

8 For previous computational studies on calcium-catalyzed reactions, see refs 4c-f and: (a) Wu, X.; Zhao, L.; Jin, J.; Pan, S.; Li, W.; Jin, X.; Wang, G.; Zhou M.; Frenking, G. Observation of Alkaline Earth Complexes $M(\text{CO})_8$ ($M = \text{Ca}, \text{Sr}, \text{or Ba}$) that Mimic Transition Metals. *Science*, **2018**, *361*, 912-916. (b) Bauer, H.; Alonso, M.; Färber, C.; Elsen, H.; Pahl, J.; Causero, A.; Ballmann, G.; De Proft F.; Harder, S. Imine Hydrogenation With Simple Alkaline Earth Metal Catalysts. *Nature Catal.* **2018**, *1*, 40-47.

9 (a) Bandini, M.; Cera, G.; Chiarucci, M. Catalytic Enantioselective Alkylations with Allylic Alcohols. *Synthesis* **2012**, *44*, 504-512. (b) Pigge, F. C. Metal-Catalyzed Allylation of Organoboranes and Organoboronic acids. *Synthesis* **2010**, *11*, 1745-1762. (c) Norsikian, S.; Chang, C. W. Control of the Regioselectivity in Palladium(0)-Catalyzed Allylic Alkylation. *Curr. Org. Synth.*, **2009**, *6*, 264-289. (d) Trost, B. M.; Van Vranken, D. L. Asymmetric Transition Metal-Catalyzed Allylic Alkylations. *Chem. Rev.* **1996**, *96*, 395-422.

10 (a) Ye, J.; Zhao, J.; Xu, J.; Mao, Y.; Zhang, Y. J. Pd-Catalyzed Stereospecific Allyl–Aryl Coupling of Allylic Alcohols with Arylboronic Acids. *Chem. Commun.* **2013**, *49*, 9761-9763. (b) Wu, H. B.; Ma, X. T.; Tian, S. K. Palladium-Catalyzed Stereospecific Cross-Coupling of Enantioenriched Allylic Alcohols with Boronic Acids. *Chem. Commun.* **2014**, *50*, 219-221.

11 Pozhydaiev, V.; Power, M.; Gandon, V.; Moran, J.; Lebœuf, D. Exploiting Hexafluoroisopropanol (HFIP) in Lewis and Brønsted Acid-Catalyzed Reactions. *Chem. Commun.* **2020**, *56*, 11548-11564.

12 (a) Negishi, E. Principle of Activation of Electrophiles by Electrophiles through Dimeric Association—Two Are Better than One. *Chem. Eur. J.* **1999**, *5*, 411-420. (b) Olah, G. A. Superelectrophiles. *Angew. Chem. Int. Ed.* **1993**, *32*, 767-788. (c) Olah, G. A., Klumpp, D. A.

Superelectrophiles and Their Chemistry. Wiley-VCH Verlag GmbH & Co. KGaA 2007. (d) Klumpp, D. A.; Anokhin, M. V. Superelectrophiles: Recent Advances. *Molecules* **2020**, *25*, 3281-3306.

13 For recent studies on the role of superelectrophiles in homogeneous catalysis, see: a) Albright, H.; Riehl, P. S.; McAtee, C. C. Reid, J. P.; Ludwig, J. R.; Karp, L. A.; Zimmerman, P. M.; Sigman, M. S.; Schindler, C.S. Catalytic Carbonyl-Olefin Metathesis of Aliphatic Ketones: Iron (III) Homodimers as Lewis Acidic Superelectrophiles. *J. Am. Chem. Soc.* **2019**, *141*, 1690-1700. b) Djurovic, A.; Vayer, M.; Li, Z.; Guillot, R.; Baltaze, J.-P.; Gandon, V.; Bour, C. Synthesis of Medium-Sized Carbocycles by Gallium-Catalyzed Tandem Carbonyl-Olefin Metathesis/Transfer Hydrogenation. *Org. Lett.* **2019**, *21*, 8132-8137. c) Albright, H.; Vonesh, H. L.; Schindler, C. S. Superelectrophilic Fe(III)-Ion Pairs as Stronger Lewis Acid Catalysts for (*E*)-Selective Intermolecular Carbonyl-Olefin Metathesis. *Org. Lett.* **2020**, *22*, 3155-3160. d) Yang, S.; Bour, C.; Gandon, V. Superelectrophilic Gallium(III) Homodimers in Gallium Chloride Mediated Methylation of Benzene: a Theoretical Study. *ACS Catal.* **2020**, *10*, 3027-3033. e) Davis, A. J.; Watson, R. B.; Nasrallah, D. J.; Gomez-Lopez, J. L.; Schindler, C. S. Superelectrophilic Aluminium(III)-Ion Pairs Promote a Distinct Reaction Path for Carbonyl-Olefin Ring-Closing Metathesis. *Nat. Catal.* **2020**, *3*, 787-796.

14 Dinda B. (2017) Group Transfer Reactions. In: Essentials of Pericyclic and Photochemical Reactions. Lecture Notes in Chemistry, Vol 93. Springer, Cham.

15 (a) Domingo, L. R.; Chamorro, E.; Perez, P. Understanding the Reactivity of Captodative Ethylenes in Polar Cycloaddition Reactions. A Theoretical Study. *J. Org. Chem.* **2008**, *73*, 4615-4624. (b) Domingo, L. R.; Perez, P. The Nucleophilicity N Index in Organic Chemistry. *Org.*

Biomol. Chem. **2011**, *9*, 7168-7175. (c) Parr, R. G.; Szentpály, L. v.; Liu, S. Electrophilicity Index. *J. Am. Chem. Soc.* **1999**, *121*, 1922-1924. For a recent example of the use of the global nucleophilicity: (d) Liu, F.; Zhu, L.; Zhang, T.; Zhong, K.; Xiong, Q.; Shen, B.; Liu, S.; Lan, Y.; Bai, R. Nucleophilicity versus Brønsted Basicity Controlled Chemoselectivity: Mechanistic Insight into Silver- or Scandium-Catalyzed Diazo Functionalization. *ACS Catal.* **2020**, *10*, 1256-1263.

16 Johnson, E. R.; Keinan, S.; Mori-Sanchez, P.; Contreras-Garcia, J.; Cohen, A. J.; Yang, W. Revealing Noncovalent Interactions. *J. Am. Chem. Soc.* **2010**, *132*, 6498-6506.

17 Gaussian 09, Revision D.01, M. J. Frisch, G. W. Trucks, H. B. Schlegel, G. E. Scuseria, M. A. Robb, J. R. Cheeseman, G. Scalmani, V. Barone, G. A. Petersson, H. Nakatsuji, X. Li, M. Caricato, A. Marenich, J. Bloino, B. G. Janesko, R. Gomperts, B. Mennucci, H. P. Hratchian, J. V. Ortiz, A. F. Izmaylov, J. L. Sonnenberg, D. Williams-Young, F. Ding, F. Lipparini, F. Egidi, J. Goings, B. Peng, A. Petrone, T. Henderson, D. Ranasinghe, V. G. Zakrzewski, J. Gao, N. Rega, G. Zheng, W. Liang, M. Hada, M. Ehara, K. Toyota, R. Fukuda, J. Hasegawa, M. Ishida, T. Nakajima, Y. Honda, O. Kitao, H. Nakai, T. Vreven, K. Throssell, J. A. Montgomery, Jr., J. E. Peralta, F. Ogliaro, M. Bearpark, J. J. Heyd, E. Brothers, K. N. Kudin, V. N. Staroverov, T. Keith, R. Kobayashi, J. Normand, K. Raghavachari, A. Rendell, J. C. Burant, S. S. Iyengar, J. Tomasi, M. Cossi, J. M. Millam, M. Klene, C. Adamo, R. Cammi, J. W. Ochterski, R. L. Martin, K. Morokuma, O. Farkas, J. B. Foresman, and D. J. Fox, Gaussian, Inc., Wallingford CT, 2016.

18 Zhao, Y.; Truhlar, D. G. The M06 Suite of Density Functionals for Main Group Thermochemistry, Thermochemical Kinetics, Noncovalent Interactions, Excited States, and Transition Elements. *Theor. Chem. Acc.* **2008**, *120*, 215-241.

19 Marenich, A. V.; Cramer, C. J.; Truhlar, D. G. Universal Solvation Model Based on Solute Electron Density and on a Continuum Model of the Solvent Defined by the Bulk Dielectric Constant and Atomic Surface Tensions. *J. Phys. Chem. B* **2009**, *113*, 6378–6396.

20 (a) Fukui, K. Formulation of the Reaction Coordinate. *J. Phys. Chem.* **1970**, *74*, 4161-4163. (b) Fukui, K. The Path of Chemical Reactions - the IRC Approach. *Acc. Chem. Res.* **1981**, *14*, 363-368.

21 Legault, C. Y. CYLview, Version 1.0b; Université de Sherbrooke, **2009** (available at: <http://www.cylview.org>).

TOC graphic

